energies

MDPI

Article

A Small-Sample Borehole Fluvial Facies Identification Method Using Generative Adversarial Networks in the Context of Gas-Fired Power Generation, with the Hangjinqi Gas Field in the Ordos Basin as an Example

Yong Liu [1], Qingjie Xu [1], Xingrui Li [1], Weiwen Zhan [1], Jingkai Guo [1] and Jun Xiao [2,*]

[1] School of Mechanical Engineering and Electronic Information, China University of Geosciences (Wuhan), Wuhan 430074, China
[2] College of Marine Science and Technology, China University of Geosciences (Wuhan), Wuhan 430074, China
* Correspondence: xj0930@cug.edu.cn

Abstract: Natural gas power generation has the advantages of flexible operation, short start–stop times, and fast ramp rates. It has a strong peaking capacity and speed compared to coal power generation, and can greatly reduce emissions of harmful substances such as sulphur dioxide. However, in practice, the accurate identification of borehole fluvial facies in the exploration area is one of the most important conditions affecting the success of gas field exploration. An insufficient number of drilling points in the exploration area and the accurate identification of lithological data features are key to the correct identification of borehole fluvial facies, and understanding how to achieve accurate identification of borehole fluvial facies when there are insufficient training data is the focus and challenge of research within the field of natural gas energy exploration. This paper proposes a borehole fluvial facies identification method applicable to the sparse sample size of drilling points, using the Sulige gas field in the Ordos Basin of China as the research object, with the drilling lithology data in the field as the sample data and the data augmentation and classification of the images through generative adversarial networks. The trained model was then validated on the Hangjinqi gas field with the same geological properties. Finally, this paper compares the recognition accuracy of borehole fluvial facies with that of other deep learning algorithms. It was verified that this research method can be applied to oil and gas exploration areas where the number of wells drilled is small and there are limited data, and that this method achieves accurate identification of borehole fluvial facies in the exploration area, which can help to improve the efficiency of oil and gas resources drilling identification to ensure the healthy development of the power and energy industry.

Keywords: borehole fluvial facies; generative adversarial networks; sulige gas field; Hangjinqi gas field

Citation: Liu, Y.; Xu, Q.; Li, X.; Zhan, W.; Guo, J.; Xiao, J. A Small-Sample Borehole Fluvial Facies Identification Method Using Generative Adversarial Networks in the Context of Gas-Fired Power Generation, with the Hangjinqi Gas Field in the Ordos Basin as an Example. *Energies* **2023**, *16*, 1361. https://doi.org/10.3390/en16031361

Academic Editor: Manoj Khandelwal

Received: 26 December 2022
Revised: 20 January 2023
Accepted: 21 January 2023
Published: 28 January 2023

1. Introduction

The exploration of natural gas resources is the material basis for the expansion of electricity services by oil and gas companies, and the exploitation of natural gas is of great importance for the development of clean energy. Sedimentary rocks, dominated by sandstones in their natural state, are good reservoirs for natural gas resources. By accurately identifying the borehole fluvial facies, the extent of sandstone distribution in the exploration area can be inferred, which can effectively improve the success rate of natural gas and other oil and gas resources.

The accurate identification of borehole fluvial facies have long been a challenge in gas exploration. The main reasons for this challenge are as follows. Firstly, the volume of drilling data in the exploration area limits the ability to directly obtain a large number of sample tags. Secondly, the complex nature of the raw lithology data obtained from drilling

makes it easy for the human eye to make mistakes in identifying the data. Finally, manually created classification sample labels are highly subjective and costly to work with. Currently, the most common method of borehole fluvial facies identification is through geological exploration by means of geological mapping and observing the orientation of contours to analyse the inventory of various rock types in the core [1]. In addition, 3D guide model analysis of the exploration location by seismic reflection techniques can also be used to analyse the location of natural gas [2,3], but this method has the disadvantage of being cumbersome and dependent on the amount of 3D data. In recent years, deep learning algorithms, with their powerful spatial data analysis capabilities, have received widespread attention in the field of oil and gas energy exploration research. In terms of borehole fluvial facies identification, the main results are currently focused on the research of discriminating neural networks. The research methods involved mainly include data mining of lithological profiles of river strata, and learning from neural networks can provide new research ideas for the rapid identification of river locations, or studying the distribution of hydrocarbons through sandstone content and stratigraphic gas content [4–7]. The identification of borehole fluvial facies is mainly achieved through the deep burial of sandstone reservoirs with non-homogeneous reservoir properties and complex lithology resulting in diverse hydrocarbon reservoir space types in sand and conglomerate formations [8–13].

This paper constructs a borehole fluvial facies identification method based on generative adversarial networks, utilizing a small sample of borehole fluvial facies data. The goal of identifying borehole fluvial facies with high accuracy has been achieved through verification of the accuracy, given a limited amount of core data. This paper learns and extracts core features from lithological data from the Sulige gas field in the Ordos Basin, Inner Mongolia, trains a large number of expanded sample data through generative adversarial networks, and validates the effect of the expanded data by classification. In order to verify the accuracy of the identification method, this paper verifies the accuracy of the method by using the spatial core data of the subsurface reservoir in the Hangjinqi gas field exploration area in the same geological formation area, collating the core profile data of Section 1 of the Permian Shihezi Formation in 69 of the drilled wells, and constructing a generative adversarial network based on the core profile sample data to complete the identification of borehole fluvial facies. The method was validated to be highly accurate and may provide new ideas and methods for the accurate identification of borehole fluvial facies in oil and gas reservoirs.

2. Methods

Generative adversarial networks consist mainly of generator and discriminator [14–16]. The data generated by the generator needs to be discriminated by a discriminator; the purpose of the generator is to approximate as closely as possible the potential distribution of the real data, and the purpose of the discriminator is to distinguish correctly between the real data and the generated data, thus maximising the accuracy of the discrimination. The structure of the generative adversarial model is shown in Figure 1.

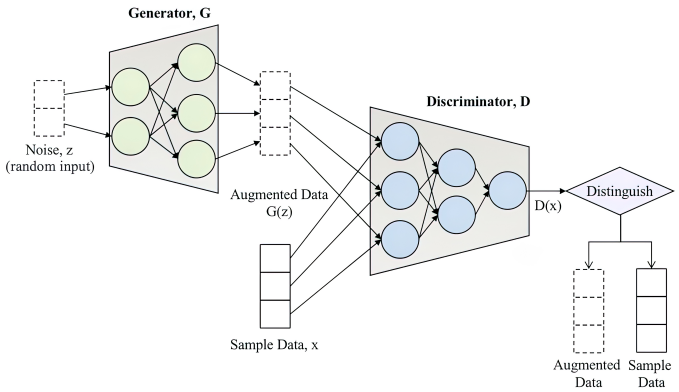

Figure 1. Traditional adversarial transfer network architecture.

The generator and discriminator in the generative adversarial network consist of separate multilayer network structures. In generative adversarial networks, noise (random input) is input to the generator, which adjusts the noise and ultimately outputs enhanced data of the same dimension as the sample lithological profile data. A data input is given to the discriminator, which may come from either amplified or sample data generated by the generator, and the output predicts and identifies whether the input data are amplified or sample data. The adversarial game in the adversarial generative model can be mathematically represented by discriminating between the discriminant function $D(x) : Rn \rightarrow [0, 1]$ and the objective function of the generative function $G : Rd \rightarrow Rn$ in terms of great minima. The generator transforms the random sample $z \in Rd$ distribution γ into the generated sample $G(z)$. The discriminator needs to distinguish it from the training samples from the distribution μ. $G(z)$ as far as possible, and the generated samples are similar in distribution to the sample data, and the target loss function of the adversarial generative network is shown below.

$$V(D, G) = E_{x\sim\mu}[logD(x)] + E_{Z\sim\gamma}[log(1 - D(G(z)))] \tag{1}$$

Its formula, E, denotes the expected value of the specified distribution in the subscript, and the description of the minimal maximal value in the generative adversarial network is shown below.

$$\min_G \max_D = E_{x\sim P_{data}(x)}[logD(x)] + E_{z\sim p_z(z)}[log(1 - D(G(z)))] \tag{2}$$

In the equation, E represents entropy, $x \sim P_{data}(x)$ represents x from the true data distribution of P_{data}, z is random noise, p_z represents the distribution of the noise, G is the discriminator, and D is the discriminator. This is because the raw numbers of the input are lithological section profile data extracted by specialisation. Considering that taking the data logarithmically does not change the relative relationship between the data, the addition of log to the equation can be used to amplify the loss and facilitate calculation and optimisation. The parameter V is found by defining a very large and very small alternating optimization.

$$\begin{aligned} V &= E_{x\sim P_{data}(x)}[logD(x)] + E_{x\sim p_G}[log(1 - D(x))] \\ &= \int_x P_{data}(x)logD(x)dx + \int_x P_G(x)log(1 - D(x))dx \\ &= \int_x [P_{data}(x)logD(x)dx + P_G(x)log(1 - D(x))]dx \end{aligned} \tag{3}$$

Equation (4) can be obtained by deriving D. It is always possible to find a good discriminator to distinguish between the real data and the generated data.

$$D^*(x) = \frac{P_{data}(x)}{P_{data}(x) + P_G(x)} \tag{4}$$

Bringing the optimal discriminator D^* into the equation of the original Generative adversarial networks, the following derivation is obtained.

$$\begin{aligned} &maxV(G, D) = V(G, D^*) \\ &= E_{x-P_{data}}[log\frac{P_{data}(x)}{P_{data}(x) + P_G(x)}] + E_{x-P_G}[log\frac{P_G(x)}{P_{data}(x) + P_G(x)}] \\ &= -2log2 + \int_x P_{data}(x)log\frac{P_{data}(x)}{(P_{data}(x) + P_G(x))/2}dx + \int_x P_G(x)log\frac{P_G(x)}{(P_{data}(x) + P_G(x))/2}dx \\ &= -2log2 + KL(P_{data}(x)||\frac{P_{data}(x) + P_G(x)}{2}) + KL(P_G(x)||\frac{P_{data}(x) + P_G(x)}{2}) \end{aligned} \tag{5}$$

By using the generator G and the trained discriminator D^* as input, the maximization formula V is obtained. Through this learning method, a distribution close to the original

data distribution can be learned, avoiding the computational complexity of the great likelihood estimation in the calculation and improving the identification effect of the discriminative model of the generative adversarial network.

Although generative adversarial networks are good at handling studies with small sample data, data volume is still the key to training identification accuracy. For this reason, in this paper, based on the traditional generative adversarial network pair, the gas field exploration data with a relatively large data volume is applied to the gas exploration area with sparse exploration data volume by a transfer learning algorithm with the expectation that the borehole fluvial facies identification method trained based on larger data volume will be applied under the same geological conditions. The main purpose of transfer learning is to take advantage of similarities between data, tasks, or models and apply models and knowledge learned in a specific domain to a new one. In this paper, the learning method based on the genesis phase of the drilled river uses an instance-based migration method, and the logical architecture of river genesis against transfer is shown in Figure 2.

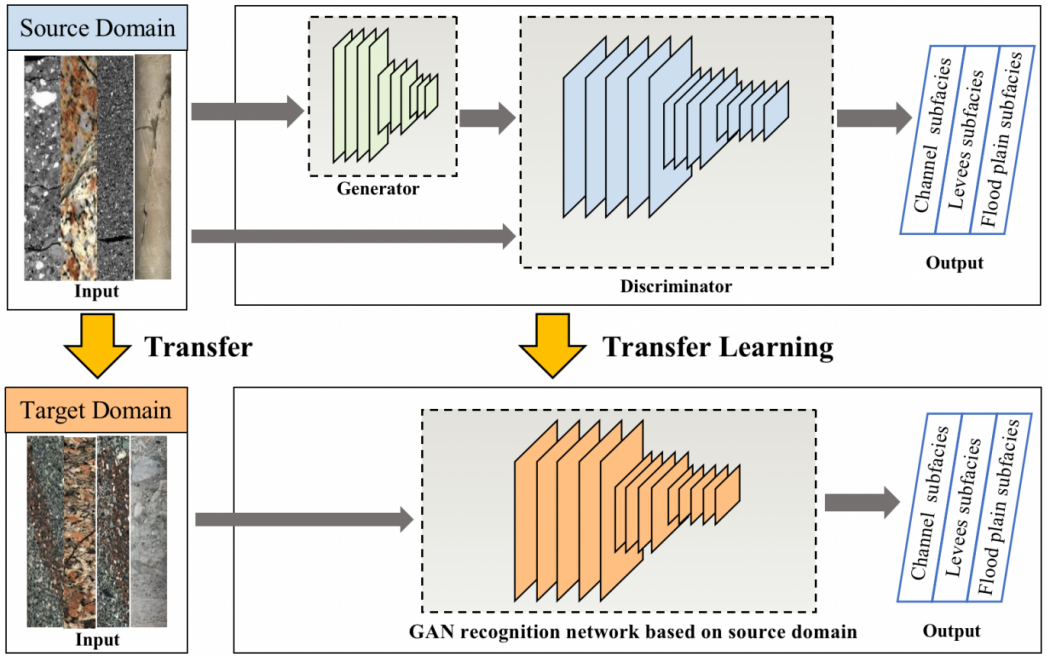

Figure 2. Adversarial transfer learning framework structure.

Borehole fluvial facies transfer learning is characterized as follows.

$$f^* = \underset{f \in H}{argmin} \frac{1}{N_s} \sum_{i=1}^{N_s} l(v_i f(x_i), y_i) + \lambda R(T(D_s), T(D_t)) \tag{6}$$

$V_i \in [0,1]$, N_S is the number of samples in the source domain, T is the feature transformation function acting on the source domain, and the sample weights V are introduced in the formula, and the mean needs to be updated to a weighted mean accordingly. In this paper, specific regularisation terms are added to the objective function of the adversarial transfer model based on borehole fluvial facies data characteristics, and under a unified representation, transfer learning is generalised to the problem of finding suitable transfer regularisation terms. The overall objective function for adversarial transfer is as follows.

$$\min_{G,C} \max_{D} L_{src}(G,C) - \frac{\lambda}{N_s + N_t} \sum_{i=1}^{N_s+N_t} L_d(D(G(x_i), d_i)) \tag{7}$$

The purpose of the input source domain data and target domain data for adversarial transfer learning is to extract domain-invariant features from the source and target domains using minimal-extreme training with the aid of the object source's conditional discriminator

(D) through the deposition layer feature extractor. $L_{src}(G, C)$ is the cross-entropy loss function for the source domain samples, and the second term is the adversarial loss, where λ is the balance parameter between the cross-entropy loss and the adversarial loss in the source domain. In addition, L_d is a dichotomous supervised cross-entropy loss function, and d_i represents the domain labels of the source and target domains, with a domain label of 0 for the source domain and a domain label of 1 for the target. The discriminator expects to distinguish as much as possible between features in the source domain and features in the target domain, while the feature extractor expects to extract the domain common features between the source and target domains to confuse the discriminator's judgement. Through the minimal great optimization of the discriminator and the feature extractor, combined with the training of the classifier, the knowledge transfer of the adversarial generative identification method of borehole fluvial facies is finally achieved.

3. Verification and Application

3.1. Case Study

Located in the north-central part of the Ordos Basin in China's Inner Mongolia Autonomous Region, the Sulige gas field has a total natural gas resource of 3.8 trillion cubic metres, has been under extensive exploration since 1999, and is relatively mature in its development [17–20]. The Hangjinqi gas field in the Inner Mongolia Autonomous Region is located to the north of the Sulige gas field and has a distinct location difference, being later than the Sulige gas field in terms of development. Exploration has revealed that box 1 of the Shihezi Formation in the Hangjinqi gas field is dominated by rocky quartz sandstone, which makes borehole fluvial facies identification more difficult due to the influence of the sandstone skeleton on logging information and the fact that the logging response of dense sandstone gas formations is different from that of conventional reservoirs. The regional location distribution of the Sulige gas field and Hangjinqi gas field is shown in Figure 3.

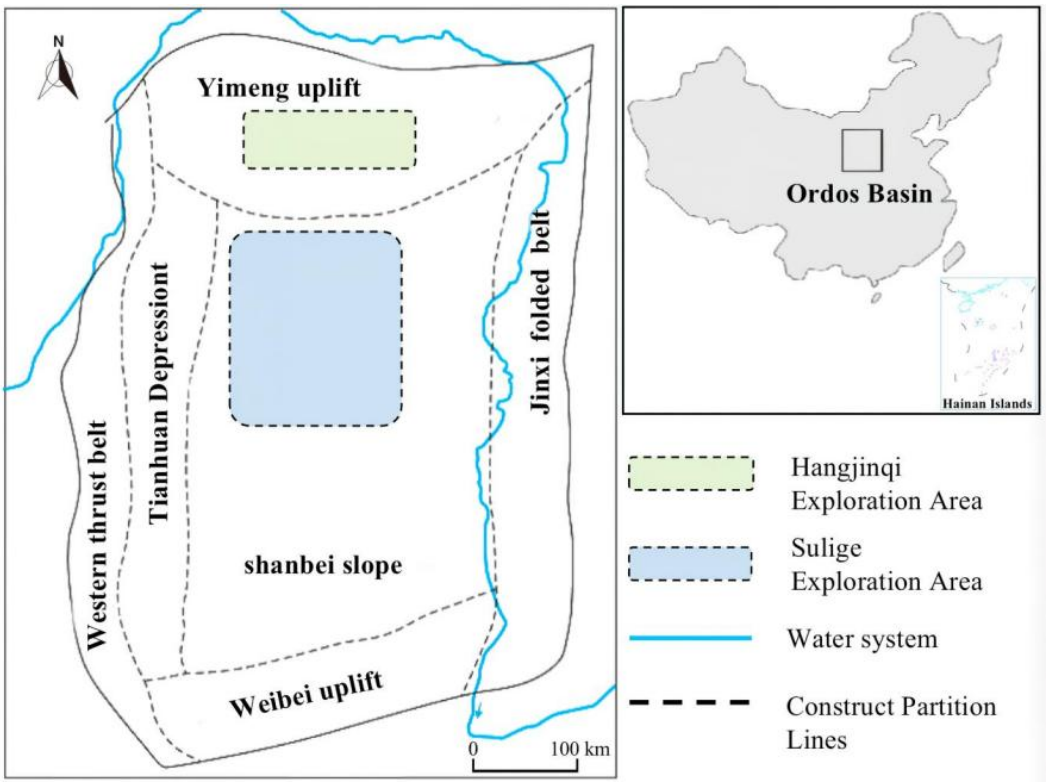

Figure 3. Classification of fluvial facies in core.

The Sulige gas field and the Hangjinqi gas field have undergone similar geological evolutionary processes and have nearly identical geological elements such as physical sources and sediment supply, which are of great comparative reference value [21,22]. In this

paper, the Sulige gas field is chosen as the source domain for data transfer and the Hangjinqi gas field as the target domain for data migration. The classification of borehole fluvial facies in the core profiles of the Sulige gas field (Shihezi formation, box 8 member) is shown in the map (Figure 4).

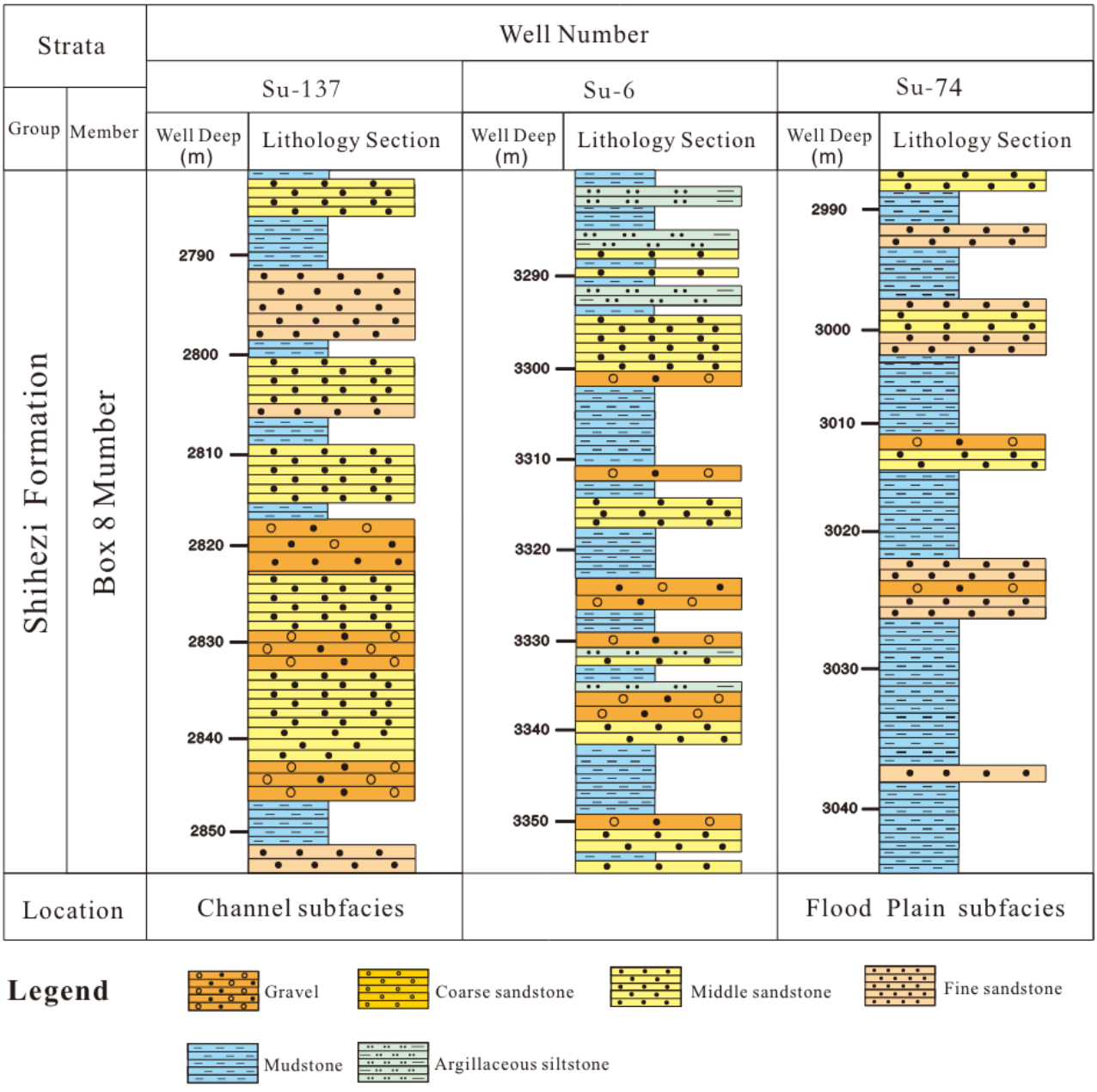

Figure 4. Classification of borehole fluvial facies in core profiles of Sulige gas field (Source domain, partial).

Since the Hangjinqi gas field was developed later than the Sulige gas field, the borehole fluvial facies data from the more mature Sulige gas field were used as the source domain to train the borehole fluvial facies identification method. Then, the trained model was applied to the borehole fluvial facies identification analysis of the Hangjin gas field. The classification of borehole fluvial facies in core profiles of Hangjinqi gas field (Shihezi formation, box 1 member) is shown in the map (Figure 5).

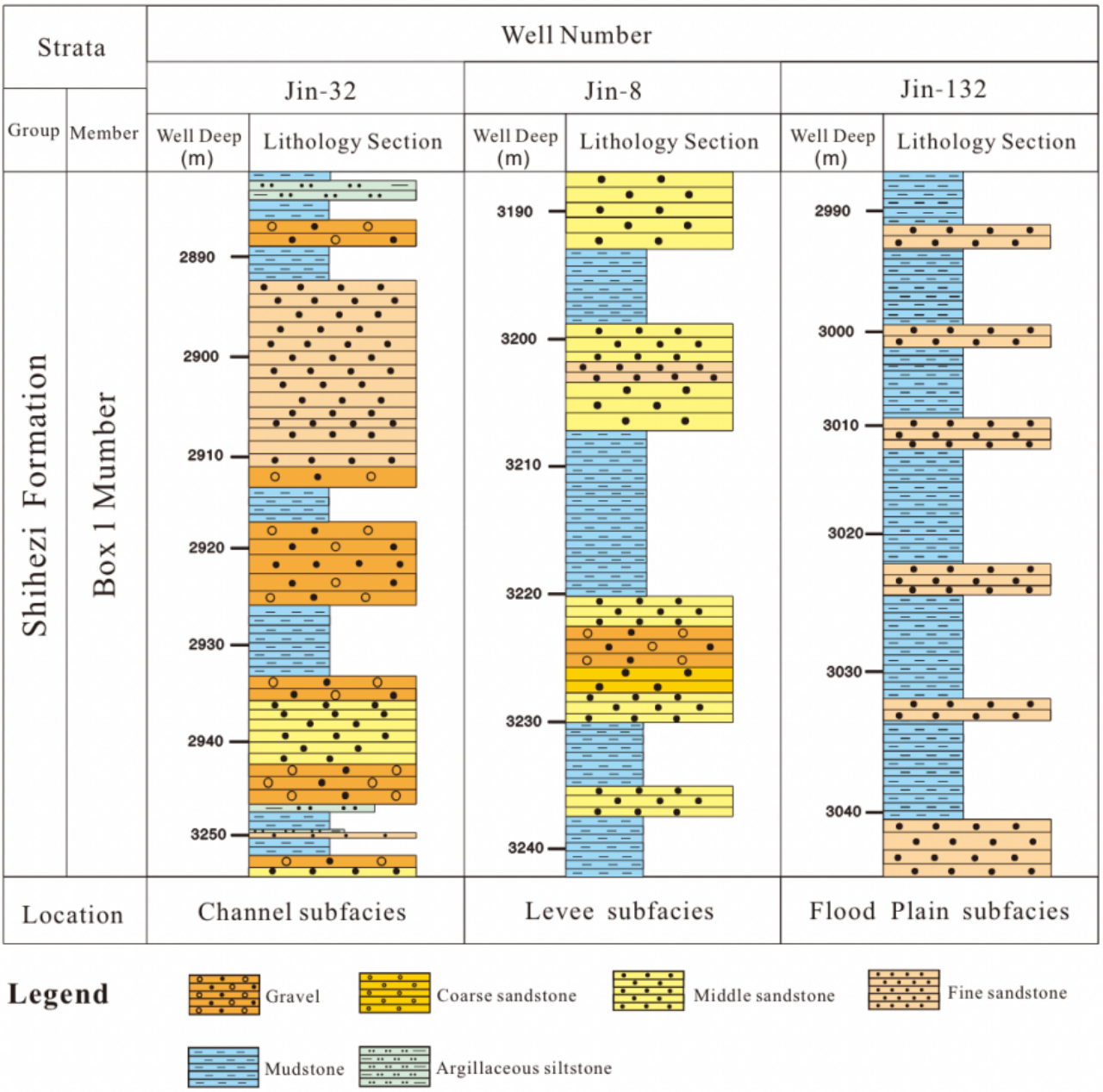

Figure 5. Classification of borehole fluvial facies in core profiles of the Hangjinqi gas field (Target domain, partial).

According to the method discussed in Section 2 of this paper, borehole fluvial facies identification learning was performed on the lithology data, and the data with near-realistic lithology profile features were trained to obtain the final identification results with high confidence through continuous training.

3.2. Borehole Fluvial Facies Identification Method

In order to obtain more accurate identification results, this paper uses alternating very large and very small optimization based on Equations (4)–(6) to find the parameters to find the optimal discriminator. A random vector of size 100 is converted to an array, and the resulting array is expanded to a $255 \times 255 \times 3$ array, using a non-linear activation function to influence the sparsity of the generative adversarial network, reducing the interdependencies between parameters and alleviating overfitting conditions. In this paper, the identification effect of landslide states is measured by accuracy and loss value. Accuracy

reflects the correct degree of state identification during training and validation, and the accuracy function is $y = a/b$, where a is the number of correct predictions and b is the total number; loss value is used to assess the degree of agreement between predicted and true values, and the formula for the loss value function is shown below.

$$H(y_{-}, y) = -\sum y_{-} * lny \tag{8}$$

where y is the predicted value and $y_{\_}$ is the true value. The discriminator network is defined as a real image and 64×64 generated images are classified. A network is created that accepts $64 \times 64 \times 3$ images, and a series of convolution layers with batch normalization is used to return a scalar prediction score to add noise to the input image. For the discriminator, the number of filters in each layer increases. Finally, according to Formulas (6) and (7), the data knowledge of the objective function for generating the countermeasure network is transferred.

3.3. Borehole Fluvial Facies: Identification of Results and Validation

With the borehole fluvial facies identification method, different types of rocks within the same geological period of sedimentation, such as fine sandstone, coarse sandstone, siltstone and mudstone, are marked differently according to the lithological data. This is to construct the borehole fluvial facies discriminator filter layer and design the discriminator based on the realisation of the lithological characteristics. Of all the monitoring data, 70% of the sample data were selected for training in generative adversarial networks and the remaining 30% were selected for validation. Based on the extracted drilling profiles for knowledge learning, the river genesis phases were classified into three categories, channel subfacies, levee subfacies, and flood plain subfaices, and the training accuracy, training loss ratio, validation accuracy, and validation loss values were compared, as shown in the figure below.

As can be seen from Figure 6, the borehole fluvial facies identification method can basically discriminate the monitoring data accurately after 30 iterations, and the borehole fluvial facies discrimination accuracy reaches 100%. The accuracy of the discriminator on the augmented data generated by the generator also increases as the number of iterations of the adversarial transfer network continues to increase, and the discrimination accuracy is as high as 97.06% at the 50th iteration. As can be seen from Figure 7, the borehole fluvial facies identification training validation loss value decreases as the number of iterations increases, and the training loss value gradually stabilises after the iterations, indicating that the identification rate of the borehole fluvial facies identification method is high and presents a low validation loss value, and the augmented data generated by the borehole fluvial facies identification method conforms to the features present in the original state data, proving the feasibility of the method to generate augmented data. As can be seen from Figure 8, the accuracy of the borehole fluvial facies identification method using monitoring data as the dataset for borehole fluvial facies category discrimination tends to stabilise after several iterations. When the borehole fluvial facies identification method uses the amplification data generated by the borehole fluvial facies generator and the monitoring data as the dataset, the discrimination accuracy of the borehole fluvial facies identification method increases with the number of iterations and reaches 80% at 50 iterations. As can be seen from Figure 9, the borehole fluvial facies identification verification loss value decreases continuously with the increase in the number of iterations and shows a decreasing trend, indicating that the borehole fluvial facies identification method has a high identification accuracy and presents a low verification loss value, which meets the requirement of the target value of the objective function and can be used for borehole fluvial facies identification.

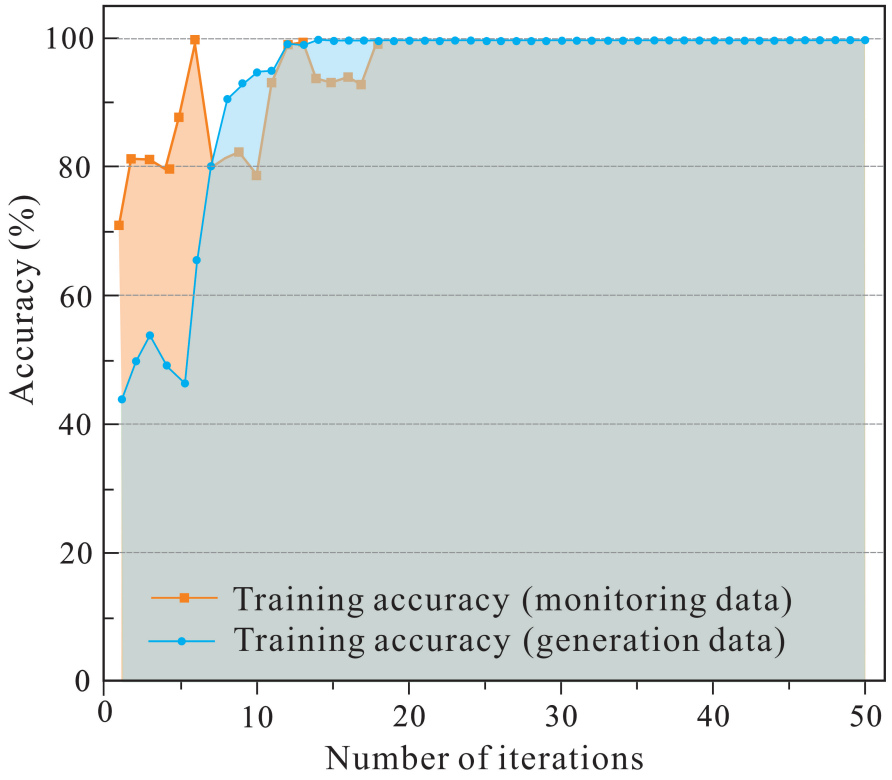

Figure 6. Training accuracy comparison.

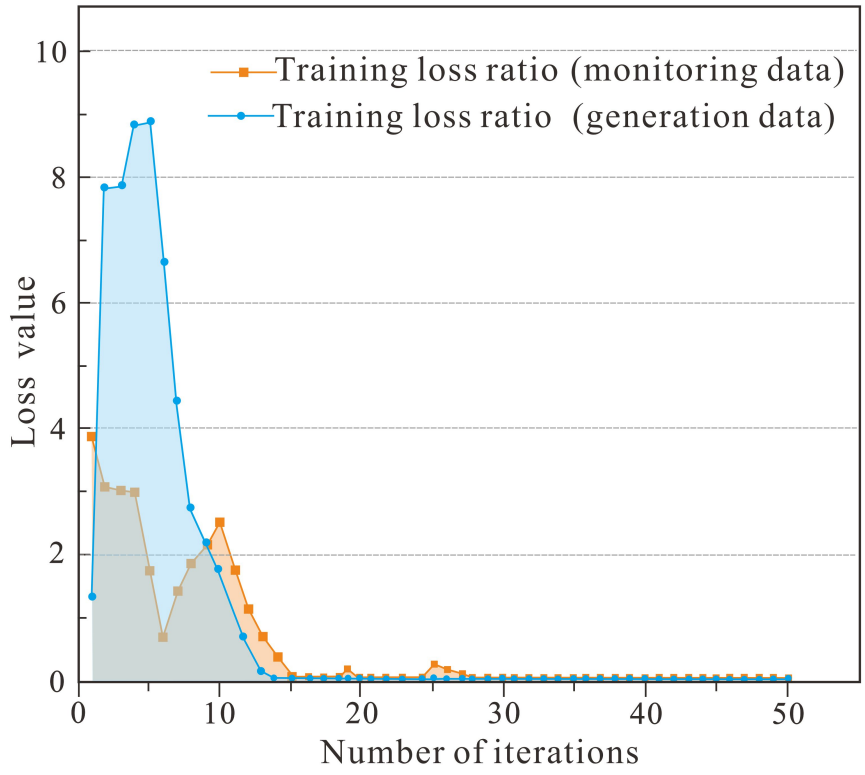

Figure 7. Training loss value comparison.

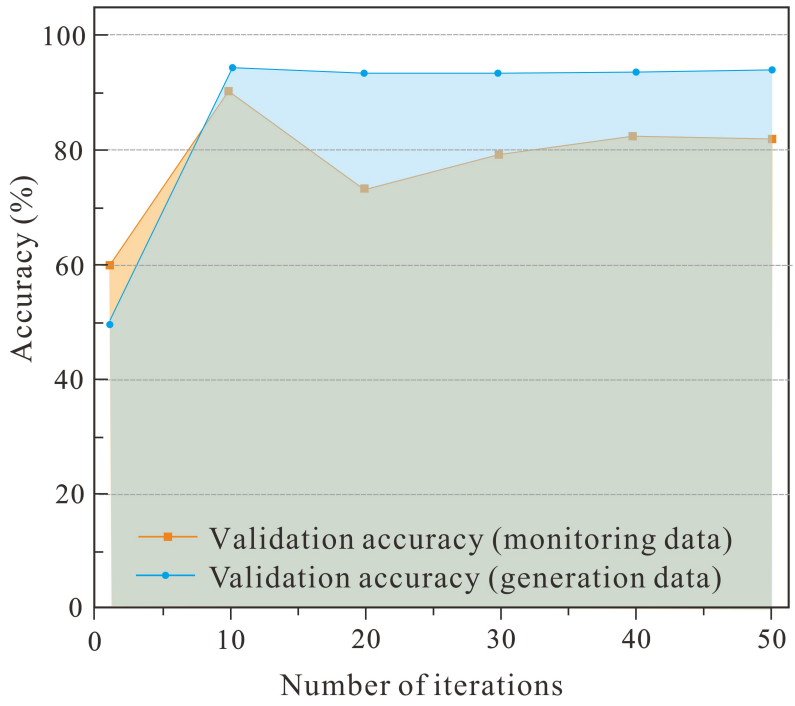

Figure 8. Verification accuracy comparison.

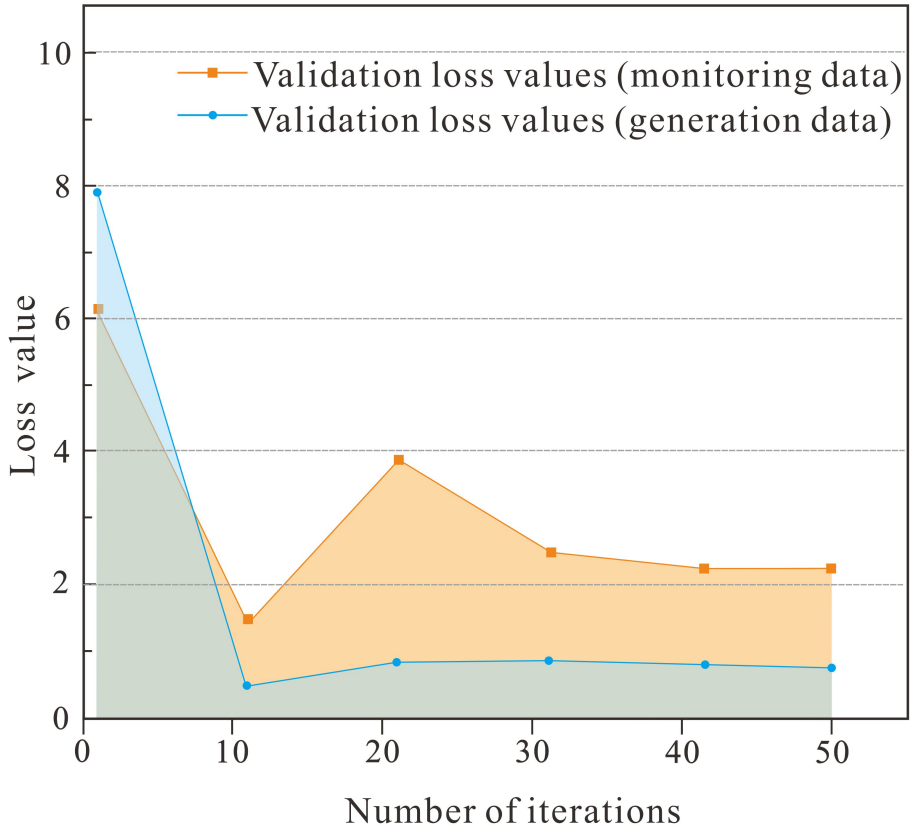

Figure 9. Verification loss value comparison.

In order to verify the training accuracy of the river genesis phase adversarial generative learning algorithm, this paper compares the training generated borehole fluvial facies generative adversarial network identification method with the K-Means algorithm [23–25]

and the convolutional neural networks learning model [26,27], respectively. The k-mean clustering algorithm is an iterative solution clustering analysis algorithm; its steps are predividing the data into K groups, then randomly selecting K objects as the initial clustering centres, followed by calculating the distance between each object and each seed clustering centre, and then assigning each object to the nearest clustering centre to it. The cluster centres and the objects assigned to them represent a cluster, and for each sample assigned, the cluster centres are recalculated based on the existing objects in the cluster, and this process is repeated until some termination condition is met. The termination condition is that the minimum number of objects is reassigned to a different cluster, no cluster centres change again, and the error sum of squares is locally minimal. The borehole fluvial facies identification process uses the core profile data as input features to the convolutional neural network and then feeds the learning data into the feedforward neural layer of the convolutional neural network, normalising the input and other two-dimensional pixel data. Convolutional neural networks rely heavily on convolutional and pooling layers to extract data features when processing data. When dealing with small sample problems, it is not possible to extract the features needed for the task from small samples through training. In contrast to k-means and convolutional neural networks, generative adversarial networks are able to process the data in a way that generates generative data that closely resemble the original data sample, following the characteristics of the real data. The algorithmic strategy using generative adversarial networks allows for a quantitative expansion of the original dataset, solving the problems caused by insufficient original data and improving recognition accuracy [28]. Table 1 shows the application of these four methods to the Hangjinqi gas field project, which are all limited by the number of wells drilled to an initial training sample size of 16. Among the four methods, the K-means and convolutional neural networks have no sample generation capability and can only use the initial 16 samples to train the relevant network, and the final result is not satisfactory. The total number of samples after the latter two methods were applied generated samples and excluded some from meeting the study requirements by means of discriminators. The total number of training samples is 961 and 856 in total, which can achieve good training accuracy at the end of training. The maximum number of iterations used in this study is the maximum number of times the algorithm converges. The convergence criterion is a general one; i.e., the recognition accuracy of the network does not change after a number of training sessions. As can be seen from Table 1, the borehole fluvial facies data learning with the transfer learning method exhibited the best results in terms of training accuracy.

Table 1. Results of the identification algorithm of the genesis of the river.

Algorithm	Total Number of Original Samples	Total Number of Training Samples after Generation of Samples	Maximum Number of Iterations	Training Accuracy
k-means	16	16 (no sample generation capability)	100	62%
convolutional neural networks	16	16 (no sample generation capability)	100	64%
borehole fluvial facies data learning without transfer learning	16	961	100	81.58%
borehole fluvial facies data learning with transfer learning	16	856	50	94.74%

Figure 10 shows a comparison of four different strategies for borehole fluvial facies identification. The vertical variables in the graph represent identification accuracy. The accuracy of each method is demonstrated for three specific borehole fluvial facies identification types, channel subfacies, levee subfacies, and flood plain subfacies.

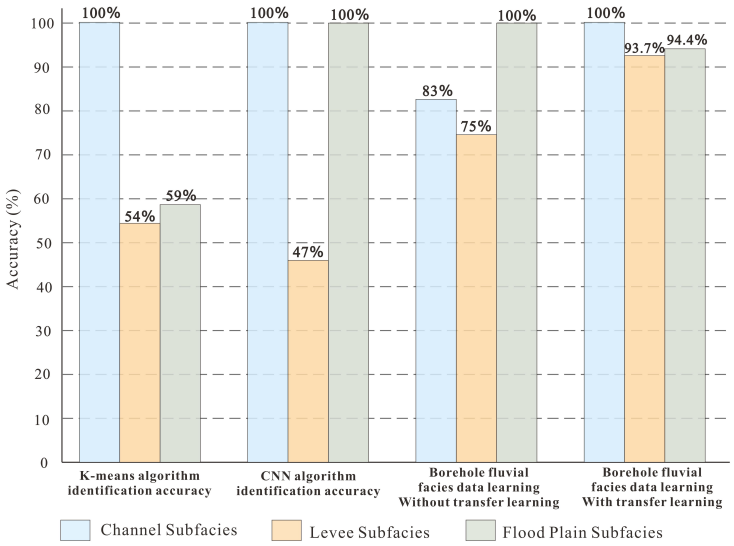

Figure 10. Comparison of algorithm identification accuracy.

Based on the results in Figure 10, it is clear that all four methods perform well in terms of channel subfacies identification accuracy. For levee subfacies identification accuracy, borehole fluvial facies data learning with transfer learning identification accuracy is the highest, and the convolutional neural networks identification accuracy is only 47%. For flood plain subfacies, all methods other than K-means achieve a high identification accuracy. In summary, it can be found that borehole fluvial facies data learning with transfer learning has a higher accuracy and reliability for borehole fluvial facies identification.

In order to verify the effectiveness of the borehole fluorescent facilities identification method in actual engineering operations, this paper compares the identification results of the borehole fluvial facies judgment identification model with the sandstone content distribution map of Hangjinqi exploration area in the scientific research project achievement report of Sinopec North China Branch, as shown in Figure 11.

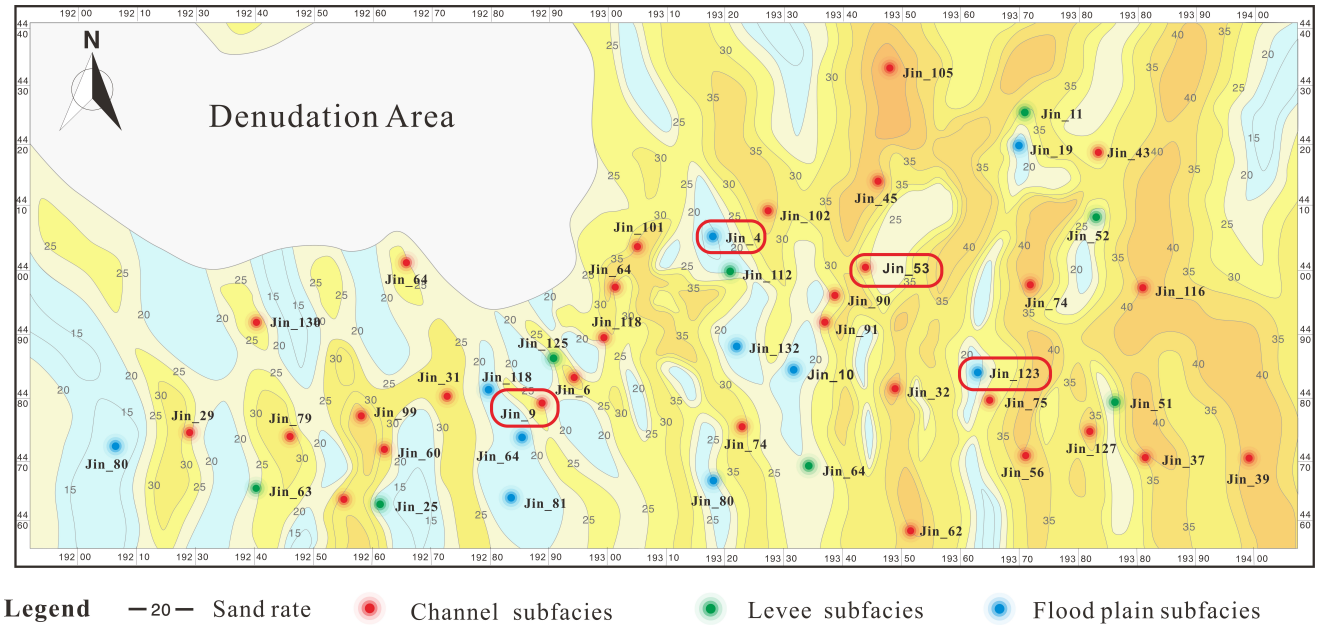

Figure 11. Borehole fluvial facies distribution map of the Hangjinqi gas field in the Ordos Basin.

In this paper, the marker information in Figure 11 is compared with the identification results of the borehole fluvial facies identification method. Based on the results of the comparison, it was found that Jin_4, Jin_9, Jin_53, and Jin_123 show significant differences. The four disputed borehole fluvial facies identification results were verified by inviting experts into the field, and according to the results, the borehole fluvial facies identification results were found to be more accurate.

The content shown in Table 2 is compared using borehole fluvial facies identification method with the borehole fluvial facies identification results from the sandstone content distribution map of the Hangjinqi gas field in the Ordos Basin produced by the project mining unit. As can be seen from Figure 11, Jin_9 and Jin_53 are misidentified channel subfacies and levee subfacies, and Jin_4 and Jin_123 are misidentified flood plain subfacies and channel subfacies. The discussion with relevant experts to identify the subfacies concluded that Jin_9 and Jin_53 are levee subfacies and Jin_4 and Jin_123 are channel subfacies with a high sandstone content.

Table 2. Location difference of channel facies sediments in a fluvial facies sand-bearing map.

Exploration Well Number	The True Location of the Identification	Position of the Markers in Figure 11
Jin_4	channel subfacies	flood plain subfacies
Jin_9	levee subfacies	channel subfacies
Jin_53	levee subfacies	channel subfacies
Jin_123	channel subfacies	flood plain subfacies

4. Discussion

This paper constructs a borehole fluvial facies identification method and validates the accuracy of borehole fluvial facies identification through generative adversarial networks, with the ultimate aim of achieving accurate identification and classification of borehole fluvial facies with a limited amount of core data.

In the borehole fluvial facies identification method, the core data can be filtered to improve the borehole fluvial facies classification accuracy and reduce the classification difficulty. However, the sample data sampling size still has an impact on the training effect of borehole fluvial facies recognition and the generation adversarial network. In addition, the method is currently studied only for natural gas fields in the same geological conditions, while the identification effect of borehole fluvial facies for natural gas fields in different geological conditions has not been verified, and the method has some limitations in terms of generalisability. Understanding how to improve the pervasiveness of borehole fluvial facies for accurate identification and the borehole fluvial facies identification method in exploration areas will be an important direction to explore in subsequent research.

The main advantage of the borehole fluvial facies identification method proposed in this paper is that it can compensate to the maximum extent for the practical situation of traditional borehole fluvial facies learning identification algorithms. This is due to the fact that this method does not require large samples of training data. The method is a good solution to the phenomenon of poor algorithm identification accuracy caused by insufficient data; it is a new research method and provides a new perspective for thinking about borehole fluvial facies feature analysis and machine identification.

5. Conclusions

The borehole fluvial facies identification method proposed in this paper is able to learn borehole fluvial facies lithology data through generative adversarial networks. It successfully applies the learning results to the borehole fluvial facies classification and identification process in the same geological conditions by extracting core features. The method has been validated to maximise the closeness of the augmented features generated by the generator network to the real sample results and significantly improves the

effectiveness and accuracy of borehole fluvial facies identification. In addition, the borehole fluvial facies identification method showed low error and high accuracy in borehole fluvial facies identification based on a small amount of sample data, indicating that the method has a good identification effect on landslide state classification. The borehole fluvial facies identification method method proposed in this paper has reference value for actual engineering practice and can be directly applied to engineering practice.

Due to the limitations of the exploration area range and stratigraphic features of natural gas fields, borehole fluvial facies identification method still has some limitations in its universality for borehole fluvial facies identification. Understanding how to further improve the universality of borehole fluvial facies identification method will be the main exploration direction for subsequent research.

Author Contributions: Y.L.: conceptualization, algorithm innovation, methodology, and writing—original draft; Q.X.: conceptualization, methodology, investigation, algorithm innovation, software, simulation, and writing—original draft; X.L.: simulation, data and formal analysis, and writing—review and editing; W.Z.: simulation, investigation, and writing—review and editing; J.G.: investigation and writing—review and editing; J.X.: original data, conceptualization, and writing—review and editing. All authors have read and agreed to the published version of the manuscript.

Funding: This research was funded by the National Natural Science Foundation of China (Grant No. 41172123 and No. 40702023).

Data Availability Statement: Data available on request from the authors.

Conflicts of Interest: The authors declare no conflict of interest.

References

1. An, Y.; Yin, X.; Gong, Q.; Li, X.; Liu, N. Classification and Provenance on Geochemical Lithogenes: A Case Study on Rock-Soil-Sediment System in Wanquan Area of Zhangjiakou, North China. *Appl. Sci.* **2023**, *13*, 8. [CrossRef]
2. Li, B.; Peng, Y.; Zhao, X.; Liu, X.; Wang, G.; Jiang, H.; Wang, H.; Yang, Z. Combining 3D Geological Modeling and 3D Spectral Modeling for Deep Mineral Exploration in the Zhaoxian Gold Deposit, Shandong Province, China. *Minerals* **2022**, *12*, 1272. [CrossRef]
3. Goswami, S.; Goswami, B.; Bhandari, G. Hexalevel Grayscale Imaging and K-Means Clustering to Identify Cloud Types in Satellite Visible Range Images. In Proceedings of the International Conference on Computational Intelligence and Computing, Vijayawada, India, 29 April 2023; Springer: Berlin/Heidelberg, Germany, 2022; pp. 13–23.
4. Capó, M.; Pérez, A.; Lozano, J.A. An efficient approximation to the K-means clustering for massive data. *Knowl.-Based Syst.* **2017**, *117*, 56–69. [CrossRef]
5. Zhang, W.; Zhu, Y.; Fu, Q. Adversarial deep domain adaptation for multi-band SAR images classification. *IEEE Access* **2019**, *7*, 78571–78583. [CrossRef]
6. Sun, W.; Liu, Z.; Davis, C.A.; Ralph, F.M.; Delle Monache, L.; Zheng, M. Impacts of dropsonde and satellite observations on the forecasts of two atmospheric-river-related heavy rainfall events. *Atmos. Res.* **2022**, *278*, 106327. [CrossRef]
7. Rashid, M.; Luo, M.; Ashraf, U.; Hussain, W.; Ali, N.; Rahman, N.; Hussain, S.; Martyushev, D.A.; Vo Thanh, H.; Anees, A. Reservoir Quality Prediction of Gas-Bearing Carbonate Sediments in the Qadirpur Field: Insights from Advanced Machine Learning Approaches of SOM and Cluster Analysis. *Minerals* **2023**, *13*, 29. [CrossRef]
8. Leila, M.; El Sharawy, M.; Bakr, A.; Mohamed, A.K. Controls of facies distribution on reservoir quality in the Messinian incised-valley fill Abu Madi Formation in Salma delta gas field, northeastern onshore Nile Delta, Egypt. *J. Nat. Gas Sci. Eng.* **2022**, *97*, 104360. [CrossRef]
9. Saito, K.; Watanabe, K.; Ushiku, Y.; Harada, T. Maximum classifier discrepancy for unsupervised domain adaptation. In Proceedings of the IEEE Conference on Computer Vision and Pattern Recognition, Salt Lake City, UT, USA, 18–23 June 2018; pp. 3723–3732.
10. Douzas, G.; Bacao, F.; Last, F. Improving imbalanced learning through a heuristic oversampling method based on k-means and SMOTE. *Inf. Sci.* **2018**, *465*, 1–20. [CrossRef]
11. Wang, F.Y. Computational experiments for behavior analysis and decision evaluation of complex systems. *J. Syst. Simul.* **2004**, *16*, 893–897.
12. Wang, F.Y. Parallel system methods for management and control of complex systems. *Control. Decis.* **2004**, *19*, 485–489.
13. Zakharov, L.A.; Martyushev, D.A.; Ponomareva, I.N. Predicting dynamic formation pressure using artificial intelligence methods. *J. Min. Inst.* **2022**, *253*, 23–32. [CrossRef]
14. Goodfellow, I.; Pouget-Abadie, J.; Mirza, M.; Xu, B.; Warde-Farley, D.; Ozair, S.; Courville, A.; Bengio, Y. Generative adversarial networks. *Commun. ACM* **2020**, *63*, 139–144. [CrossRef]

15. Finn, C.; Christiano, P.; Abbeel, P.; Levine, S. A connection between generative adversarial networks, inverse reinforcement learning, and energy-based models. *arXiv* **2016**, arXiv:1611.03852.
16. Ran, X.; Xue, L.; Sang, X.; Pei, Y.; Zhang, Y. Intelligent Generation of Cross Sections Using a Conditional Generative Adversarial Network and Application to Regional 3D Geological Modeling. *Mathematics* **2022**, *10*, 4677. [CrossRef]
17. Wang, F.; Gao, C. Settlement–river relationship and locality of river-related built environment. *SAGE J.* **2020**, *29*, 10. [CrossRef]
18. Shen, J.; Qu, Y.; Zhang, W.; Yu, Y. Wasserstein distance guided representation learning for domain adaptation. In Proceedings of the AAAI Conference on Artificial Intelligence, New Orleans, LA, USA, 2–7 February 2018; Volume 32.
19. Wu, X.; Liang, L.; Shi, Y.; Geng, Z.; Fomel, S. Multitask learning for local seismic image processing: Fault detection, structure-oriented smoothing with edge-preserving, and seismic normal estimation by using a single convolutional neural network. *Geophys. J. Int.* **2019**, *219*, 2097–2109. [CrossRef]
20. McDaniel, P.; Papernot, N.; Celik, Z.B. Machine learning in adversarial settings. *IEEE Secur. Priv.* **2016**, *14*, 68–72. [CrossRef]
21. Szegedy, C.; Zaremba, W.; Sutskever, I.; Bruna, J.; Erhan, D.; Goodfellow, I.; Fergus, R. Intriguing properties of neural networks. *arXiv* **2013**, arXiv:1312.6199.
22. Ye, R.; Cha, Y.H.; Dickens, T.; Vdovina, T.; MacDonald, C.; Denli, H.; Liu, W.; Kovalski, M.; som de Cerff, V. Multi-channel convolutional neural network workflow for automatic salt interpretation. In Proceedings of the SEG International Exposition and Annual Meeting, OnePetro, San Antonio, TX, USA, 15–20 September 2019.
23. Liu, M.Y.; Tuzel, O. Coupled generative adversarial networks. *arXiv* **2016**, arXiv:1606.07536.
24. Pan, S.J.; Yang, Q. A survey on transfer learning. *IEEE Trans. Knowl. Data Eng.* **2010**, *22*, 1345–1359. [CrossRef]
25. Gössling, S.; Cohen, S.; Higham, J.; Peeters, P.; Eijgelaar, E. Desirable transport futures. *Transp. Res. Part D Transp. Environ.* **2018**, *61*, 301–309. [CrossRef]
26. Pant, D.; Bista, R. Image-based Malware Classification using Deep Convolutional Neural Network and Transfer Learning. In Proceedings of the 2021 3rd International Conference on Advanced Information Science and System (AISS 2021), Sanya, China, 26–28 November 2021; pp. 1–6.
27. Han, S.; Yang, F.; Jiang, H.; Yang, G.; Wang, D.; Zhang, N. Statistical analysis of infrared thermogram for CNN-based electrical equipment identification methods. *Appl. Artif. Intell.* **2022**, *36*, 2004348. [CrossRef]
28. Liang, B.; Wang, Z.; Si, L.; Wei, D.; Gu, J.; Dai, J. A Novel Pressure Relief Hole Recognition Method of Drilling Robot Based on SinGAN and Improved Faster R-CNN. *Appl. Sci.* **2022**, *13*, 513. [CrossRef]